Biomaterials 225 (2019) 119533

Contents lists available at ScienceDirect

Biomaterials

journal homepage: www.elsevier.com/locate/biomaterials

Ex vivo culture of adult CD34$^+$ stem cells using functional highly porous polymer scaffolds to establish biomimicry of the bone marrow niche

C.E. Severn[a,b], A.M. Eissa[c,d,e], C.R. Langford[f], A. Parker[a], M. Walker[g], J.G.G. Dobbe[h], G.J. Streekstra[h], N.R. Cameron[d,f], A.M. Toye[a,b,*]

[a] School of Biochemistry, Biomedical Sciences Building, University of Bristol, Bristol, BS8 1TD, UK
[b] National Institute for Health Research Blood and Transplant Research Unit (NIHR BTRU) in Red Blood Cell Products, University of Bristol, UK
[c] Department of Polymers, Chemical Industries Research Division, National Research Centre, El Bohouth St. 33, Dokki, Giza, 12622, Cairo, Egypt
[d] School of Engineering, University of Warwick, Coventry, CV4 7AL, UK
[e] Department of Chemistry, University of Warwick, Coventry, CV4 7AL, UK
[f] Department of Materials Science and Engineering, Monash University, Clayton, 3800, Victoria, Australia
[g] Department of Physics, University of Warwick, Coventry, CV4 7AL, UK
[h] Amsterdam UMC, University of Amsterdam, Department of Biomedical Engineering and Physics, Meibergdreef 9, Amsterdam, the Netherlands

ARTICLE INFO

Keywords:
Three-dimensional
Erythroid
Scaffold
polyHIPE
Haematopoietic
Jagged-1
Functionalisation

ABSTRACT

Haematopoiesis, the process of blood production, occurs from a tiny contingent of haematopoietic stem cells (HSC) in highly specialised three-dimensional niches located within the bone marrow. When haematopoiesis is replicated using *in vitro* two-dimensional culture, HSCs rapidly differentiate, limiting self-renewal. Emulsion-templated highly porous polyHIPE foam scaffolds were chosen to mimic the honeycomb architecture of human bone. The unmodified polyHIPE material supports haematopoietic stem and progenitor cell (HSPC) culture, with successful culture of erythroid progenitors and neutrophils within the scaffolds. Using erythroid culture methodology, the CD34$^+$ population was maintained for 28 days with continual release of erythroid progenitors. These cells are shown to spontaneously repopulate the scaffolds, and the accumulated egress can be expanded and grown at large scale to reticulocytes. We next show that the polyHIPE scaffolds can be successfully functionalised using activated BM(PEG)$_2$ (1,8-bismaleimido-diethyleneglycol) and then a Jagged-1 peptide attached in an attempt to facilitate notch signalling. Although Jagged-1 peptide had no detectable effect, the BM(PEG)$_2$ alone significantly increased cell egress when compared to controls, without depleting the scaffold population. This work highlights polyHIPE as a novel functionalisable material for mimicking the bone marrow, and also that PEG can influence HSPC behaviour within scaffolds.

1. Introduction

Most if not all cells in the body reside in a 3D environment where an array of cell signals, extracellular matrix, cytokine and chemokine signalling are likely presented simultaneously and are tightly regulated. The bone marrow is an example of such a complex 3D environment, where the human body efficiently compartmentalises the multi-stage process of haematopoiesis. Here, normal blood production occurs continually at an impressive rate, using only a tiny contingent of haematopoietic stem cells for an individual's entire lifetime. This contrasts to current state of the art planar two-dimensional (2D) liquid cultures, where the process of erythropoiesis is routinely replicated in a laboratory setting using culture systems that have been optimised over 15–20 years. To date, 2D culture systems have generated a dose of 2.5 mL packed reticulocytes to provide a proof of principal autologous transfusion into a single patient [1] and more recently stirrer flask cultures have generated 10 mL volume of leukofiltered packed reticulocytes [2]. Although the cell numbers produced by erythroid 2D cultures are impressive, nutrients, cytokines and growth factors are provided in excess and in a relatively uncontrolled fashion, reducing cellular expansion potential. These limitations to the current 2D culture process mean that the manufacture of a standard adult therapeutic dose in the region of 2×10^{12} cRBCs remains an extensive bioengineering and logistical challenge.

A wide range of materials have been utilised for the engineering of biomimetic materials for 3D culture of haematopoietic lineages to try and better reflect the *in vivo* situation, with examples including; polyurethane (PU) [3–6], fibrin [7], bio-derived bone [8], poly(ethylene

* Corresponding author. School of Biochemistry, Biomedical Sciences Building, University of Bristol, Bristol, BS8 1TD, UK.
E-mail address: ash.m.toye@bristol.ac.uk (A.M. Toye).

https://doi.org/10.1016/j.biomaterials.2019.119533
Received 3 April 2019; Received in revised form 26 September 2019; Accepted 28 September 2019
Available online 04 October 2019

terephthalate (PET) [9], non-woven polyester disks [10], hollow fibres [11] and also the incorporation of hydrogels either alone or in combination with other porous scaffold materials [12–16]. As well as offering the potential to compartmentalise cell proliferation and differentiation and control cellular growth signals, scaffold cultures have a range of additional potential benefits over 2D culture, including the reduction of media volumes via an increase in surface area and a reduction in the use of cytokines if scaffolds are biomimetic, both of which would offer a reduction in costs. In addition, 3D cultures have the potential for self-perpetuation of stem cells by more accurate control of growth factors and stimuli and also an accompanied reduction in labour requirements (as discussed in Ref. [17]). The successful biomimicry of the bone marrow niche using scaffold cultures would offer a wide range of potential uses, including tissue engineering for blood production, models systems for fundamental stem cell research on steady state haematopoiesis and haematopoietic disease, in addition to medical applications such as HSC expansion for transplants and as a drug screening platform.

We have previously shown successful biocompatibility and culture of adult $CD34^+$ haematopoietic stem and progenitor cells (HSPCs) in PU scaffolds but this scaffold system was largely exhausted after 28 days of continued culture and egress [6]. We now describe a second-generation scaffold based culture system employing a thiol-containing biomimetic polyHIPE scaffold to enable functionalisation of the material surface for *ex vivo* expansion of HSPCs. Polymerised high internal phase emulsions (polyHIPEs) are produced by emulsion templating whereby the continuous, oil-based phase of the emulsion is polymerised in the presence of the aqueous phase droplets, yielding a highly porous solid foam material [18–23]. The scaffold type was switched from PU to polyHIPE for two reasons; 1) polyHIPEs can be prepared with pendant thiol (-SH) functionality allowing easy attachment of molecules of interest; and 2) polyHIPE scaffolds currently have proven biocompatibility and performance in a range of *in vitro* 3D cell culture systems including; osteoblasts [24,25], HepG2 liver cells [26], neurons [27,28], adipocyte derived stem cells [29], neural progenitor cells [30] and primary human endometrial cells [31]. The successful biomimicry of the bone marrow niche microenvironment would facilitate sustainability and maintenance of the stem cell pool; ultimately increasing the retention and expansion of the seeded $CD34^+$ population. Functionalisation of scaffold materials offers a means of presenting cells with absent niche signals not currently provided *ex vivo*. PolyHIPE scaffolds have successfully demonstrated efficacy of surface functionalisation with galactose and acrylic acid for the culture of hepatocytes [32,33]. More recently polyHIPE scaffolds have been functionalised with fibronectin to enhance adhesion of human endometrial cells to scaffold materials [34].

This study describes for the first time, the utility of a polyHIPE scaffold material for prolonged haematopoietic stem and progenitor cell (HSPC) culture. We demonstrate retention of HSPCs for 28 days within the compartmentalised scaffold but also continuous egress and re-occupation. The accumulated cell egress from the polyHIPE scaffolds can also act as a seed for erythroid large-scale liquid cultures, producing significant numbers of reticulocytes. We then explore the post-polymerisation functionalisation of the polyHIPE scaffold using a $BM(PEG)_2$ linker and peptide. Although we did not observe any effect of the specific peptide used, we did observe a proliferative effect of the $BM(PEG)_2$ linker, illustrating it is possible to increase output further via PEG functionalisation whilst still retaining proliferative cells within the scaffold. Therefore, porous polyHIPE scaffolds represent an exciting novel system for potentiation of a compartmentalised haematopoietic seed culture, and their ease of functionalisation provides the foundation for biomimicry of the bone marrow niche.

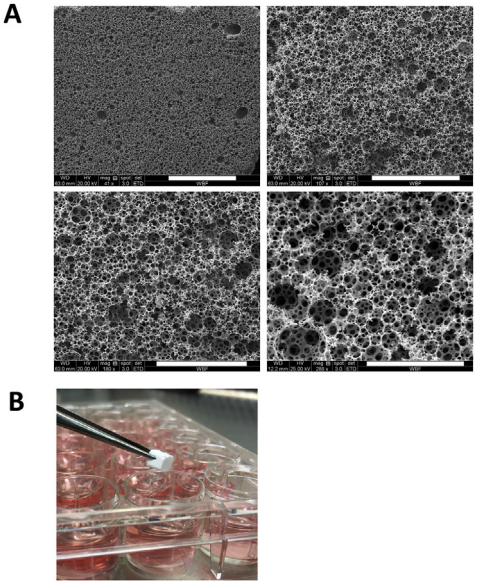

Fig. 1. Demonstration that polyHIPE scaffolds mimic the human bone marrow honeycomb architecture. A) Scanning electron micrographs (SEM) of polyHIPE scaffolds at a range of magnifications including 41× (top left), 107× (top right), 180× (bottom left) and 288× (bottom right). Scale bars for images are as follows; 41× (1 mm), 107× (500 μm), 180× (300 μm), 288× (200 μm). B) Photograph of polyHIPE scaffolds (5 mm × 5 mm) being moved into a fresh well of media.

2. Results

2.1. Properties of polyHIPE scaffold material

Scaffold fabrication is described in detail within the materials and methods. Briefly, scaffolds were prepared using a HIPE oil phase, consisting primarily of dipentaerythritol penta-/hexa-acrylate (DPEHA) and trimethylolpropane tris(3-mercaptopropionate), producing an inter-connected, compartmentalised foam-like scaffold with a structure resembling that of human bone (Fig. 1a). PolyHIPE scaffolds with a dimension of 0.5 cm by 0.5 cm cubed were found to have a nominal porosity of between 80 and 90% and average pore diameters ranging from 10 to 130 μm (Supplemental Fig. 1c). The scaffolds produced for this study therefore had an average pore diameter of 37 ± 19 μm [31,35–37].

Compression tests were performed and the resulting stress-strain curves were produced (Supplemental Fig. 1a). Materials displaying classical rigid foam behaviour have curves with an initial linear elastic region followed by a plateau. At small strains, usually less than ca. 10%, the linear elastic region has a slope equal to the compression (Young's) modulus. At higher loads, the foam cells (voids) begin to collapse under the applied load giving a stress plateau. The compressive Young's moduli values for the unfunctionalised polyHIPE materials were found to be 13.85 ± 7.13 KPa (Supplemental Fig. 1b) and were able to recover their original dimensions after compression.

2.2. Utilising polyHIPE scaffolds for the expansion of haematopoietic lineages

The use of these scaffolds for the *ex vivo* culture of a range of haematopoietic lineages was explored via directed differentiation towards the erythroid, macrophage and neutrophil lineages, in addition to bone marrow-derived mesenchymal stem cells (MSCs, as previously described [38]) (Supplemental Fig. 2). The scaffolds were sectioned to determine internal cellular occupation, this showed erythroid and neutrophil suspension cultures had a propensity to grow and

differentiate from the CD34$^+$ cells seeded within the material. Occupation of the scaffold was also increased in the polyHIPE structure after 28 days compared to our previously published work culturing erythroid lineage cells in PU scaffolds; where distribution and population was sparse in comparison (Supplemental Figs. 3d and 6). In contrast CD14$^+$ selected macrophage cultures remained on the seeding surface with sparse and superficial population of the material. Bone marrow MSCs also largely remained on the seeding edge of the scaffold.

2.3. PolyHIPE scaffolds for the long-term culture of the erythroid lineage

Next, we focused on the ability of the scaffolds to support HSC and erythroid lineage growth. Scaffolds were seeded statically, as described previously [6] using 0.5×10^6 CD34$^+$ cells isolated from adult peripheral blood mononuclear cells (PBMNCs) and maintained in serum-free expansion medium for 28 days. Complete media changes were carried out every second day by carefully moving the scaffold into a fresh well of media (Fig. 1b). The number of cells that exited the scaffold into the surrounding medium, termed the cell egress, was used as a measure of the scaffold capacity to support proliferation. This revealed an average peak of cell production at day 14 (4.57×10^5 cells) and a total of 2.85×10^6 cells egressed on average for the entire culture period (Fig. 2a). Supplemental Fig. 3 provides images for comparison to our previously published scaffold culture using PU scaffolds and the current polyHIPE scaffolds [6]. Cell egress across 28 days is comparable with polyHIPE cultures peaking on day 14, which is 4 days later than PU cultures, although total cell egress is comparable (Supplemental Fig. 3a and b). Cell death for polyHIPE cultures was reduced across the culture period compared to PU cultures demonstrating favourable conditions for cell proliferation (Supplemental Fig. 3c).

When cell egress populations were assessed using a flow cytometry surface marker panel developed previously [6], there was a persistence of CD34$^+$ cells throughout the culture, albeit decreasing in population size and mean fluorescence intensity (MFI) post day 8 of culture and progressively towards the culture endpoint (Fig. 2b and Supplemental Fig. 5). A prominent and increasing CD36 expression profile was observed, indicative of megakaryocyte and erythroid progenitors (MEPs) and early erythroid progenitors [39–41]. Whilst a CD34$^+$/CD36$^+$ cell represents an MEP a CD34$^+$/CD36$^-$ expressing cell is indicative of a less committed stem cell; as expected there is a large CD34$^+$/CD36$^-$ population early in the culture which then decreases, however interestingly

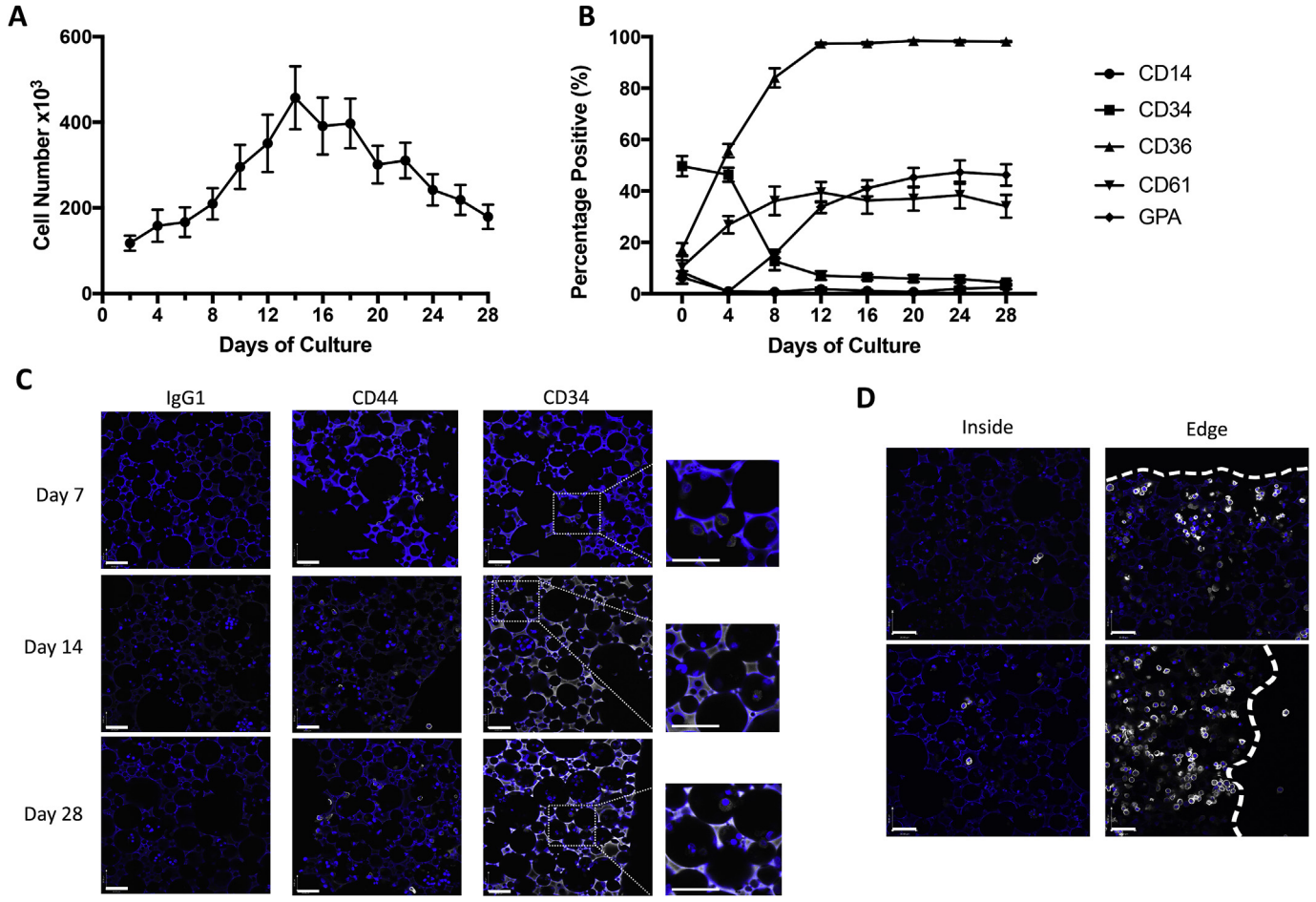

Fig. 2. PolyHIPE scaffold cultures are able to progress for 28 days where a large proportion are early erythroid progenitors. A) Cellular egress every second day from control polyHIPE cultures over a 28-day period. Cells counts were conducted using the MACSQuant flow cytometer with automated addition of propidium iodide to exclude dead cells. B) Flow cytometry analysis on egress from polyHIPE cultures were assessed every 4 days using the MACSQuant flow cytometer with antibodies to detect the following populations; CD14 (FITC), CD34 (VioBlue), CD36 (PE), CD61 (APC-Vio770) and GPA (APC) as a single flow cytometry panel. Cellular populations are shown as a percentage of the total live cell population. C) Expression of CD44 and CD34 throughout the polyHIPE scaffold culture period. Scaffolds were embedded in paraffin and 10 μm sections cut from approximately the middle of the scaffold at days 7 (top), 14 (middle) and 28 (bottom) of the culture. A CD34 (BirmaK3) or CD44 (Bric 235) antibodies were applied to sections neat or IgG1 control and then coupled to Alexa 647 donkey anti-mouse secondary antibody (displayed in white in the images); DAPI was used to stain the nucleus. Inlays highlight CD34$^+$ expression within the scaffolds. D) GPA expression at the edge or centre of the scaffold, GPA (Bric 256) was used to stain scaffold sections at day 28 of culture. Images were captured using the 60× lens, all scale bars are 30 μm. N = 4 in triplicate, error bars represent the standard error of the mean.

there was a second wave of $CD34^+/CD36^-$ generated around day 20 of culture (Supplemental Fig. 5d). In comparison to CD36, the increase in glycophorin A (GPA) expression was more moderate both in terms of percentage population and MFI, confirming that cell egress population represents early erythroid progenitors (Fig. 2b and Supplemental Fig. 5). CD61 expression in scaffold egress cells remains moderate but consistent throughout the culture suggesting that scaffolds enable maintenance of an early stage of lineage commitment and differentiation (Fig. 2b) [42–45]. Finally, CD14 was also included to detect monocytes and macrophages however this population remained largely absent.

Scaffolds were also fixed, embedded in paraffin wax, sectioned on the indicated days of culture and probed with lineage markers (Fig. 2c and d). Using CD44, a pan haematopoietic marker, expression was observed throughout the structure revealing full penetration and population of the material. CD34 was also present, demonstrating the retention of the seeded population and also confirming the flow cytometry data that expression reduces whilst persisting until the culture endpoint. Interestingly, a large proportion of the internal cell population was observed to reside at the edge of the scaffold highly expressing GPA (Fig. 2d). Taken together, these data suggest that the scaffold is acting to selectively to retain certain populations of HSCs allowing the persistence and continued proliferation of the culture, albeit through unknown mechanisms at present. Importantly, the population of the polyHIPE scaffold was considerably increased over our first-generation PU scaffold particularly at the edges; therefore, demonstrating a propensity for the material to retain HSPCs (Supplemental Fig. 3d).

2.4. PolyHIPE scaffolds offer a favourable three-dimensional environment

To further investigate the observation of the higher cell density at the very edge of scaffold, we first explored the behaviour of cells in scaffolds after seeding with $CD34^+$ cells as above and then imaged over 3 days to visualise cell egress. Targeted locations in the well plate were repeatedly imaged using the Incucyte Zoom imagining system. This revealed that cells exit and accumulate in areas surrounding the scaffold (Supplemental Fig. 6a), in addition Supplemental Fig. 6b demonstrates the cells accumulate around the scaffold over a 3-day period. This raised the question of whether egressed cells also re-enter the scaffold between full media changes. To test this, an experiment using an empty “follow on” scaffold was devised (Fig. 3a). Control scaffolds were seeded as described above and moved to a new well of media every two days, a second empty scaffold was placed into this media vacated by the first scaffold which contained the egressed cells. This process continued for a total of 16 days. Quantification of internal cell populations either at the centre or the edge of the scaffold demonstrated that the scaffolds offer an environment favourable to cells compared to medium. However, perhaps unsurprisingly, the difference in cellular abundance between seeded and originally non-seeded scaffolds was found to be significant ($P = \leq 0.05$) and highly significant ($P = \leq 0.0001$) for the centre and edge of the scaffold respectively (Fig. 3b and c). Therefore, the repopulation of empty scaffolds suggests the polyHIPE material is offering a favourable environment over liquid culture.

We next hypothesised that proteins from the media were being adsorbed onto the surface of polyHIPE scaffolds and subsequently presented to cells. Proteomic assessment of proteins attached to the surface of the material during the equilibration step (containing 10% FCS) revealed 348 proteins across 3 repeats after multiple stringent washes with a boric acid buffer. When the data was analysed for relative abundance the top 20 proteins are displayed in Fig. 3d and include; haemoglobin, serotransferrin, transferrin and thrombospondin.

2.5. Cell egress can be expanded and grown at scale

To understand the proliferative potential of scaffold cultures, cumulative cell egress was grown in a traditional 2D liquid culture using spinner flasks. To initiate these cultures a single scaffold was seeded as above, placed within a final volume of 40 mL of serum free media in a static tissue culture flask and then incubated for 14 days. Total scaffold egress on day 14 was transferred to a spinner flask in medium to support erythroid differentiation (Fig. 4a). On day 14 cells were largely $CD36^+GPA^+$ erythroid progenitors with little CD34 persisting when assessed using flow cytometry (Fig. 4b). When expanded and differentiated in spinner flasks for a further 12 days, a total of $(2.59 \pm 0.212) \times 10^9$ cells were grown from the egress of a single scaffold. This post-scaffold expansion generated a total fold increase of 5.18×10^3 from the initial seeded material. Upon filtration with a leukofilter removing nuclei and nucleated cells, a total of $(4.21 \pm 0.344) \times 10^8$ reticulocytes remained (Fig. 4c). The deformability of the reticulocytes produced was tested using an automated rheoscope and cell analyser (ARCA) [46]. In comparison to mature RBC the reticulocyte product deformability was remarkably similar, although as expected the spinner flask reticulocytes had a larger area than the RBCs (Fig. 4d and Supplemental Fig. 7) consistent with their being reticulocytes rather than mature RBCs. Preliminary data suggests that additional expansion from the scaffold culture cells that egress between 14 and 28 days is possible, albeit with a lower reticulocyte yield (data not shown).

2.6. Functionalisation of polyHIPE scaffolds using a $BM(PEG)_2$ linker

Thiol-acrylate polyHIPE materials with residual free thiols on the surface were first reacted with $BM(PEG)_2$, forming a stable thio-ether bond at one end [36,47]. The other end can then act as a handle for subsequent reactions with cysteine-containing moieties, providing a facile route to post-polymerisation surface functionalisation, in this case with Jagged-1 peptides (reported previously [48]) which possess three cysteine residues (schematic, Fig. 5a). Functionalisation of polyHIPE scaffolds with $BM(PEG)_2$ and Jagged-1 peptide was monitored using x-ray photoelectron spectroscopy (XPS) to determine the atomic surface composition (Fig. 5b and Supplemental Fig. 8d). The survey spectra of $BM(PEG)_2$ and Jagged-1 peptide-functionalised scaffolds display N1s peaks at ca. 399 eV, whereas the unfunctionalised scaffold had no peaks in the N1s region, as expected (Supplemental Fig. 8a–c). The high-resolution N1s spectra displayed an increase in nitrogen peak intensity when Jagged-1 peptide was covalently attached to the $BM(PEG)_2$-functionalised scaffolds, confirming successful functionalisation (Fig. 5c and d). The second component observed in the N1s spectra at ca. 402 eV is believed to be due to the limited quaternisation side reactions of amine/amide functionalities during the functionalisation reaction.

The effect of functionalisation on the rigidity of the material was tested using Young's Modulus. $BM(PEG)_2$ functionalised scaffolds gave a Young's modulus of 44.03 ± 24.45 KPa compared to control scaffolds of 13.85 ± 7.13 KPa (Supplemental Fig. 1b). Therefore, the $BM(PEG)_2$ functionalisation significantly ($P = < 0.05$) increased the rigidity of the material and showed irreversible deformation. On the other hand, the unfunctionalised material is relatively flexible and could recover almost completely after compression, retaining their original dimensions.

2.7. Functionalisation of scaffolds with $BM(PEG)_2$ increases cell egress compared to controls

To test for the effect of functionalisation on cell egress, four different scaffolds were used; a control scaffold, $BM(PEG)_2$ functionalised scaffold, Jagged-1 peptide functionalised scaffold and a scrambled Jagged-1 peptide functionalised scaffold. Cell egress was assessed over 20 days from control, Jagged-1 and scrambled Jagged-1 scaffolds and all were found to be comparable. In contrast $BM(PEG)_2$ functionalised scaffolds demonstrated a significant increase in overall scaffold egress between days 6 and 12, where for example on day 12 the average cell

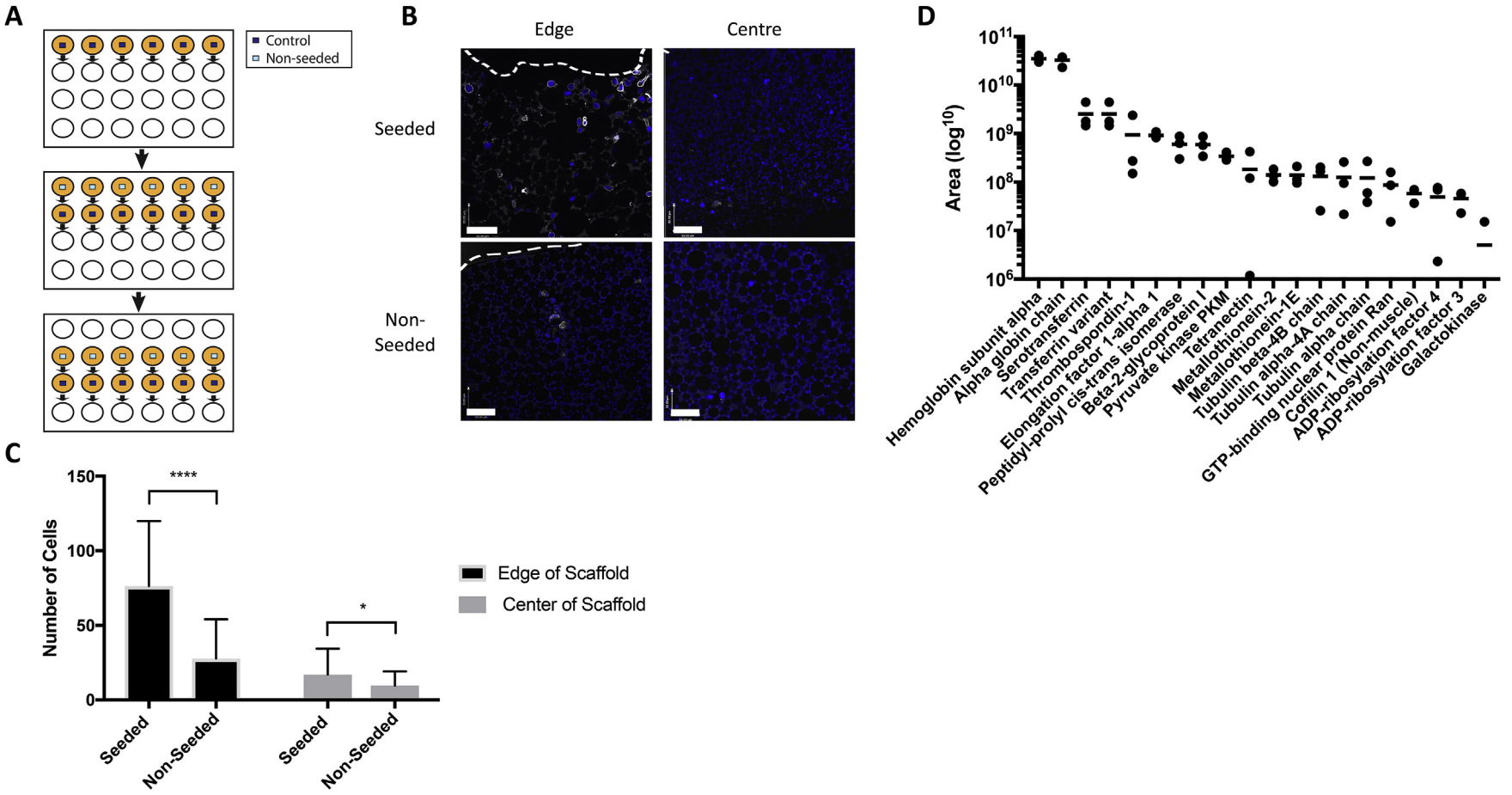

Fig. 3. PolyHIPE scaffolds offer an environment with a propensity to attract cells. A) Schematic depicting the movement of control scaffolds followed by non-seeded scaffolds for 16 days testing whether egress cells move back into the scaffolds. B) Scaffolds were seeded (or not seeded at all) with 0.5×10^6 $CD34^+$ cells and were cultured in serum free expansion media for 16 days. GPA (Bric 256) antibody was applied to scaffold sections neat and then coupled to Alexa 647 donkey anti-mouse secondary antibody (displayed in white in the images); DAPI was used to stain the nucleus. Images were captured using the 60× lens, scale bars are 33 μm. C) Quantification of cells in seeded and non-seeded polyHIPE scaffolds using DAPI staining. Image J software was used for quantification and a Students *t*-test used to test for significance where * P = < 0.05, ****P = < 0.0001. D) Mass spectrometry analysis of surface serum proteins deposited during scaffold equilibration before cell seeding. Data are represented as a comparison of area. N = 3 and scale bars represent the standard error of the mean.

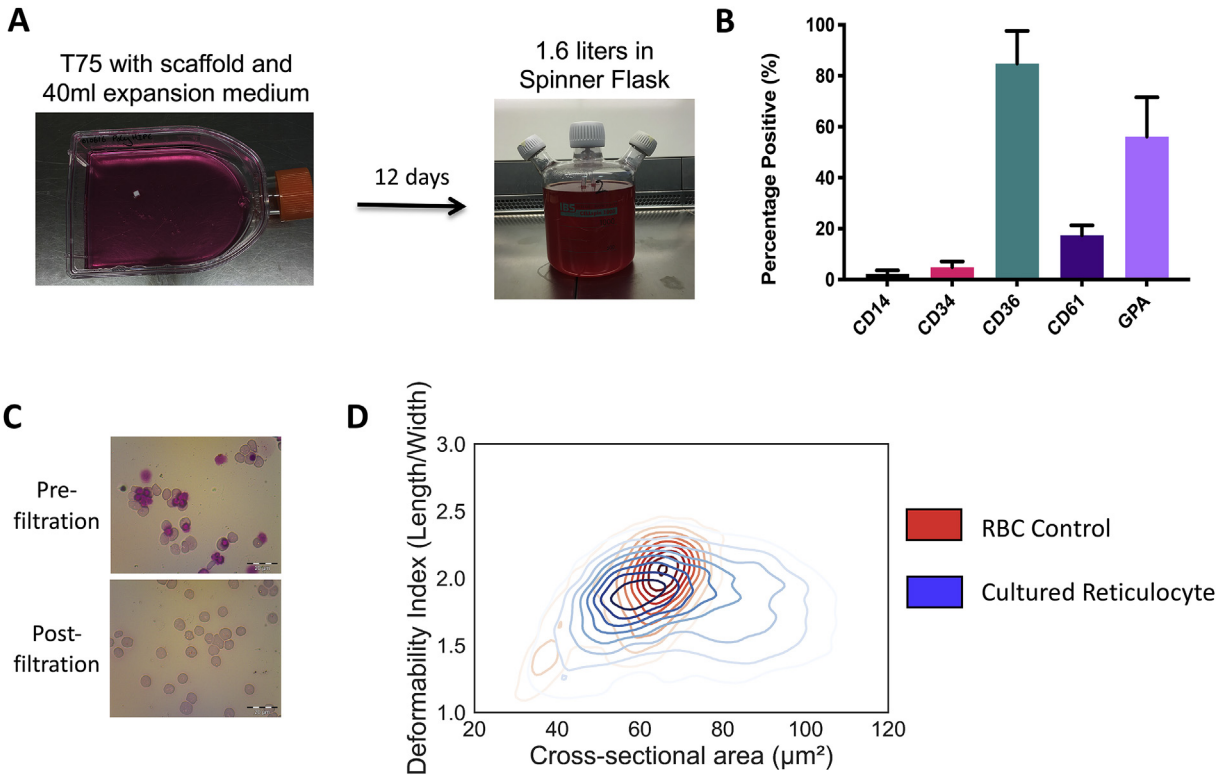

Fig. 4. PolyHIPE cultures can be used as a starter for large-scale liquid cultures. A) Photographs of the scaffold culture and then spinner flask culture. B) Flow cytometry analysis on egress from polyHIPE cultures were assessed on day 14 before transition to the spinner flask using the MACSQuant flow cytometer with antibodies to detect the following populations; CD14 (FITC), CD34 (VioBlue), CD36 (PE), CD61 (APC-Vio770) and GPA (APC). Cellular populations are shown as a percentage of the total live cell population, dead cells were excluded using propidium iodide. C) Cytospin images of cells pre and post leukofiltration. Cells were cytospun onto slides and stained with May-Grünwald's and Giemsa stains before viewing. D) Comparison of size (x-axis) and deformability (y-axis) for control native RBCs (in red) and cultured reticulocytes (in blue). N = 3, error bars represent the standard error of the mean. (For interpretation of the references to colour in this figure legend, the reader is referred to the Web version of this article.)

egress for $BM(PEG)_2$ scaffolds were 5.43×10^5 and 1.92×10^5 for control scaffolds. When assessed as total cell egress across the entire culture this difference was highly significant ($P = < 0.001$, Fig. 6a and b) when compared to control scaffolds. It should be noted here that the control scaffolds presented alongside functionalisation data were produced separately to those in Fig. 2, possibly explaining differences in cell egress. Differences in cell surface expression in populations over the culture period between the scaffolds was minimal, suggesting that BM

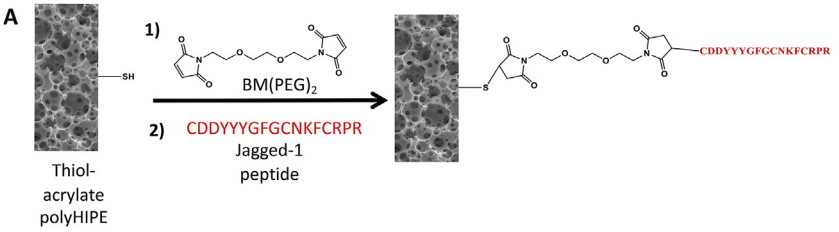

B

Overall composition of N1s (atomic %)	
Unfunctionalised polyHIPE	0
$BM(PEG)_2$-funcationalised polyHIPE	1.74
Jagged-1 peptide-funcationalised polyHIPE	9.55

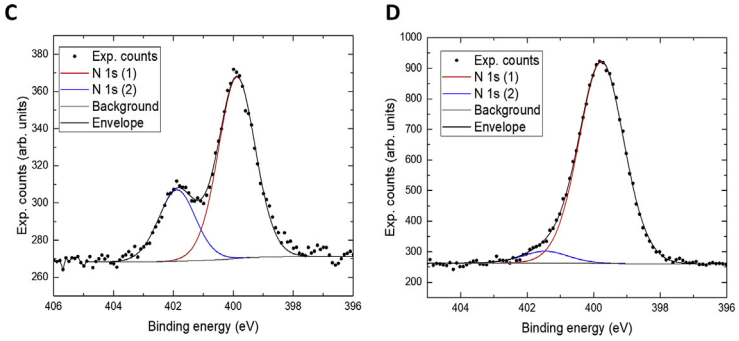

Fig. 5. Functionalisation of polyHIPE scaffolds using $BM(PEG)_2$, successful functionalisation assessed using XPS. A) Schematic representation of the surface functionalisation of polyHIPE scaffolds. B) Atomic composition of N1s from XPS data of polyHIPE scaffolds. Atomic percentages are accurate to ± 2%. XPS high-resolution peak-fitted N 1s spectra for c) $BM(PEG)_2$ and d) Jagged-1 peptide functionalised polyHIPE scaffolds. Component 1 (red) amide/imide, component 2 (blue) quaternary amine/amide/imide (N^+R_4). (For interpretation of the references to colour in this figure legend, the reader is referred to the Web version of this article.)

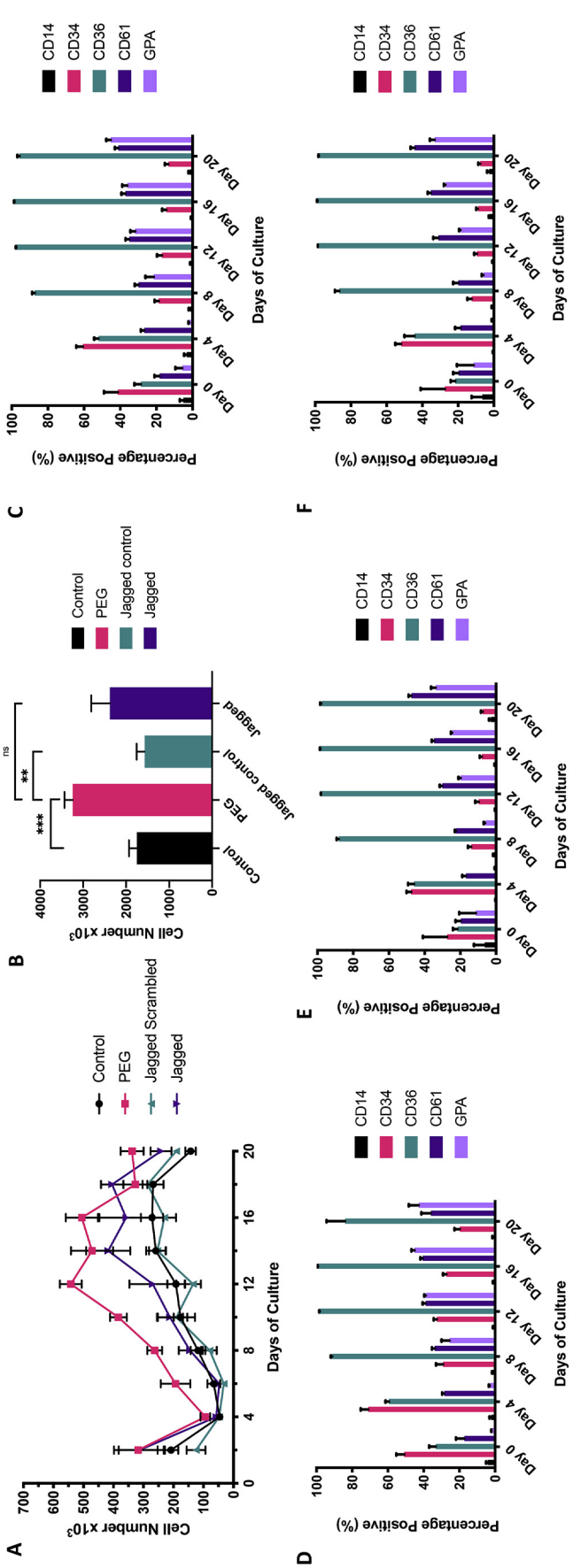

Fig. 6. BM(PEG)$_2$ polyHIPE scaffolds increase cell egress from scaffolds but does not influence cell phenotype. A) Cellular egress from functionalised polyHIPE cultures. Cells counts were conducted using the MACSQuant flow cytometer with automated addition of propidium iodide to exclude dead cells. Cellular egress from control, BM(PEG)$_2$ cross linked scaffolds, jagged scrambled and jagged polyHIPE scaffolds every second day over a 20-day period. B) Cumulative cell egress from Fig. 6a. C,D,E and F) Flow cytometry analysis on egress from C) control D) BM(PEG)$_2$ functionalised scaffolds E) Jagged scrambled F) Jagged polyHIPE cultures were assessed every 4 days using the MACSQuant flow cytometer with antibodies to detect the following populations; CD14 (FITC), CD34 (VioBlue), CD36 (PE), CD61 (APC-Vio770) and GPA (APC). Cellular populations are shown as a percentage of the total live cell population, dead cells were excluded using propidium iodide. A minimum of 30 000 events were captured per sample. ***P = < 0.001, **P = < 0.01.

$(PEG)_2$ or peptide attachment did not alter cell lineage commitment and differentiation in scaffold cell egress (Fig. 6c–f). The expected increase in the $CD34^+$ population in the Jagged-1 scaffolds over controls was not observed and cell populations within the scaffold were also comparable upon immunofluorescence labelling of scaffold sections using CD34 and GPA as markers (Supplemental Fig. 9).

3. Discussion

This study has shown the propensity of polyHIPE scaffolds to mimic the compartmentalisation observed in honeycomb structures of the bone marrow and their biocompatibility for prolonged *ex vivo* culture of HSCs. Unlike our previously reported PU based scaffolds [6] we have demonstrated that the HSPCs still occupy the scaffolds extensively after 28 days of culture, whereas the PU based scaffolds are mostly exhausted by this stage of culture. The scaffolds utilised here for HSPC cultures perform best with $CD34^+$ derived erythroid and neutrophil cultures, whereas adherent cells such as macrophages and MSCs did not persist within the scaffold in its current design. Scaffold occupation was particularly favourable for erythroid cultures with $CD34^+$ cells proliferation potential remaining within the scaffold and also egress from each individual 0.5 cm^3 scaffold persisting for the 28 days of culture. For the first time we also show that with this material the cells that egress do not simply just remain outside of the scaffold but re-enter the scaffolds, populating the edges and also deeper within the scaffolds, demonstrating an attraction of cells to the material. Proteomic studies found that protein adsorption from the media equilibration step occurs onto polyHIPE scaffolds, which may also enhance the scaffolds attraction for certain cell types such as HSPCs.

We show that the erythroid progenitors that spontaneously exit polyHIPE scaffolds are highly proliferative, with an average of a 5.18×10^3 fold increase in total cell number generated in post scaffold liquid culture. This demonstrable capacity for scaffolds to successfully seed larger scale liquid culture systems whilst still retaining an internal population, is a unique and novel benefit of the protocol and system as a whole. Although not described in this work an additional 2-week period of expansion from scaffold egress was also possible but proliferative capacity of the egressed cells reduced with continued culture. Further optimisation work would be required to ensure cells are correctly maintained in the appropriate media to match the differentiation stage, offering potential to further improve the reticulocyte yield and proliferation achieved by the cells that egress later. This preliminary scale-up data also demonstrates the exciting versatility and potential of the scaffold system should self-renewal be induced further by functionalisation.

True *ex vivo* biomimicry requires scaffolds to be functionalised, presenting absent *in vivo* signals, aiding in proliferation or facilitation of a cellular phenotype. In an attempt to increase the proliferation of $CD34^+$ cells within polyHIPE scaffolds used here, we presented absent bone marrow niche signals using the notch signalling pathway by functionalising scaffolds with Jagged1 peptides via a $BM(PEG)_2$ linker. There is current evidence of notch signalling to support and increase the self-renewal of $CD34^+$ cells and HSPCs *in vitro* in 2D and 3D culture systems. Lee et al. has provided evidence for the use of Jagged-1 ligand for the expansion of HSCs and production of T cells using a layer by layer surface modification method on inverted colloidal crystal scaffolds [49]. Further work by Benveniste demonstrated $CD34^+$ cell expansion *in vitro* was also supported by OP-9 cells expressing delta like-4 notch ligand, although notch signalling was not a requirement in the *in vivo* experiments [50]. More recently delta-1 ligand has been immobilised on microparticles in stirred bioreactors to increase progenitor cell numbers [51] and incorporated into PEG containing hydrogels for the expansion of umbilical cord $CD34^+$ derived T cells [52]. Unfortunately, in our system the Jagged-1 peptide used did not offer a significant increase in cell egress nor an elevated $CD34^+$ scaffold population when compared to control cultures. One explanation could be that the peptide is presented in a non-bioactive manner, as there are 3 cysteine residues in the peptide, any of which could react with the BM $(PEG)_2$. Therefore, the peptide is likely to be presented in multiple orientations to the cells. Another explanation is that the peptide itself does not exert a bio-active enhancement effect in our culture conditions or when immobilised. In our study Jagged-1 peptide was immobilised covalently, whereas the original study which published the peptide sequence used the peptide in solution [48].

Interestingly, the $BM(PEG)_2$ linker alone provided a positive proliferative effect, with significantly increased scaffold cellular egress observed compared to the unfunctionalised control scaffolds. When the mechanical behaviour of the scaffolds was tested under compression, the $BM(PEG)_2$ scaffolds were significantly more rigid compared to unfunctionalised scaffolds. The increase in rigidity of the $BM(PEG)_2$ functionalised material, more closely reflecting that of the endosteal niche at 35KPa may account for the difference in cell behaviour [53–56]. The response of the scaffold population to the change in microtopography and biomaterial mechanostimulus may encourage the subsequent proliferation within the cultures [57–59] (reviewed in Refs. [60,61]). This effect, however, could also be due to $BM(PEG)_2$ functionalisation causing the material to be more hydrophilic thus improving cell migration, medium flow and nutrient exchange. This proliferative effect did not occur when $BM(PEG)_2$ was added into 2D liquid cultures suggesting that it is not a result of the direct effect of the molecule (data not shown).

Applications of PEG are versatile and in the past have included surgical implant coating [62], polymer-based drug delivery [63] and incorporation into hydrogels for tissue engineering [13–16]. As a result of such work, PEG has been included in the fabrication or functionalisation of hydrogels and scaffolds material fabrication for many years partly owing to its versatile properties [13–16]. Our data therefore strengthens the evidence for inclusion of PEG in HSC $CD34^+$ scaffold cultures and in particular as a novel scaffold modification to drive proliferation.

Although we show here for the first-time enhancement of proliferation and egress using PEG functionalisation of polyHIPE scaffolds, a more biomimetic functionalisation of the scaffolds would offer a facile route to increase the complexity of current three-dimensional cultures and thus *ex vivo* biomimicry of the bone marrow niche. However, only a limited degree of biomimetic expansion has been observed previously and the field is still exploring factors that regulate HSCs. To this end, we are currently screening a peptide library for suitable HSC expansion and maintenance candidates, before transitioning into the established scaffold model. A culture system that successfully and comprehensibly recapitulates and mimics the human bone marrow niche would offer benefits further afield than simply a seed source for large scale cultures and the production of reticulocytes for transfusion. Such a system would have utility as a broad and powerful research tool for exploring haematopoiesis in health and disease and for therapeutic applications including for example, the expansion of HSCs for subsequent stem cell transplantation or drug screening. This study therefore presents polyHIPE as a novel and functionalisable scaffold biomaterial for the culture and manipulation of HSCs *ex vivo*.

4. Materials and methods

4.1. Antibodies

Primary antibodies, Bric 235 (CD44 40 μg/mL, IBGRL reagents), Birma K3 (CD34 40 μg/mL, IBGRL reagents) and Bric 256 (GPA 97 μg/mL, IBGRL Reagents) were used undiluted on scaffold sections. Conjugated antibodies; CD36, CD61, GPA, CD34 (Miltenyi Biotec) CD14 (BioLegend) were all used as per manufacturer's instructions. Alexa Fluor 647 (Invitrogen) was used as a secondary antibody for immunofluorescence studies at 5 μg/mL.

4.2. Peripheral blood mononuclear cell and CD34$^+$ cell isolation

Peripheral blood mononuclear cells (PBMNC) were isolated from platelet apheresis blood waste (NHSBT, Bristol, UK) from healthy donors with informed consent. Ethics approval for all experimental protocols was granted by Bristol Research Ethics Committee (REC 12/SW/0199), and all methods were carried out in accordance with approved guidelines. PBMNC separation was performed using Histopaque® 1077 as described previously [64,65]. CD34$^+$ and CD14$^+$ cells were isolated from PBMNCs using magnetic activated cell separation (MACS, Miltenyi Biotec) as previously described and according to manufacturer's instructions [65–67].

4.3. Scaffold preparation

The preparation of polyHIPE materials by emulsion templating and photopolymerisation has been previously reported [36]. Briefly, polyHIPE scaffolds of 90% nominal porosity were prepared as follows: the HIPE oil phase, consisting dipentaerythritol penta-/hexa-acrylate (DPEHA; 3.47 g), trimethylolpropane tris(3-mercaptopropionate) (TMPTMP; 4.84 g), 1,2-dichloroethane (DCE; 7 mL), surfactant hypermer B246; 0.50 g, and a photoinitiator (a blend of diphenyl(2,4,6-trimethylbenzoyl)-phosphine oxide and 2-hydroxy-2-methylpropiophenone; 0.7 mL) was added to a 2-neck round bottom flask and light was excluded. An aqueous phase of deionised water (126 mL) was then added dropwise with constant shear (300 rpm) from an overhead stirrer fitted with a D-shaped PTFE paddle. Once addition of the aqueous phase was complete, the HIPE was stirred for a further minute in order to ensure emulsion homogeneity. The HIPE was then poured into a syringe, then added to a (0.5 × 0.5 × 0.5) cm PTFE mould and cured by passing under a UV irradiator (Fusion UV Systems Inc. Light Hammer 6 variable power UV curing system with LC6E benchtop conveyor), producing cubical polyHIPE monoliths. Once cured, the polyHIPE was then washed by immersion in acetone, followed by Soxhlet extraction in dichloromethane overnight. The polyHIPE was then dried under reduced pressure. The produced polyHIPE material has been shown to possess residual surface thiols [47]. These thiols can then be used as a handle to allow post-polymerisation functionalisation with maleimides, via Michael addition under benign conditions [68]. PolyHIPE scaffolds have the additional benefit that they are manufactured in a mould, increasing standardisation and therefore the reproducibility between scaffold experiments and also ability for scale-up of the system.

4.4. Compression testing

The mechanical behaviour of polyHIPE materials under compression was evaluated using a Shimadzu EZ-LX compact table-top universal tester equipped with a 500 N load cell fitted with compression plates tested at ambient temperature. The polyHIPE samples were cubes of 0.5 mm in dimension. Compression was continued until a final strain of around 50% was reached. Experiments were repeated using six different samples of each material to obtain average Young's modulus values.

4.5. Scaffold void measurement

Image analysis was carried out using Image J image analysis software (version 1.49). Void diameters of 100 voids were measured in a random walk across the SEM micrograph. A statistical correction factor is applied to the data in order to account for the underestimation in void diameter [69].

4.6. Functionalisation with BM(PEG)$_2$

30 cubes of polyHIPE scaffolds (ca. 200 mg) were placed in a glass vial containing a solution of BM(PEG)$_2$ (70 mg) in 1,2-dichloromethane (DCM; 20 mL). A 100 μL of trimethylamine (TEA) was added and the mixture was left at ambient temperature for 48 h. The polyHIPE scaffolds were washed with DCM (3 × 5 mL) and ethanol (3 × 5 mL).

4.7. Functionalisation with Jagged-1 peptide

12 cubes of polyHIPE scaffolds (ca. 85 mg) were placed in a vial containing a solution of 25 mg Jagged-1 peptide, CDDYYYGFGCNKFCRPR or jagged control peptide, CRGPDCFDNYGRYKYCF (published previously [48]) in 50% aqueous ethanol (20 mL). 50 μL of TEA was added and the mixture was left at ambient temperature for 48 h. The polyHIPE scaffolds were finally washed with ethanol (3 × 10 mL). Jagged-1 amino acid sequence was reordered to produce a scrambled to use as a peptide control for the addition of a peptide to the scaffold.

4.8. X-ray photoelectron spectroscopy

X-Ray photoelectron spectroscopy (XPS) analysis was performed using a Kratos Axis Ultra DLD spectrometer at the University of Warwick. The scaffolds were cut to suitable size, attached to double sided carbon tape and mounted onto a stainless-steel bar. The surface composition of the modified scaffolds was characterised. The data was subsequently charge corrected using the C–C/C–H peak at 284.6 eV as a reference. The measurements were conducted at room temperature and at a take-off angle of 90° with respect to the surface. Survey spectra were acquired to determine the elemental composition of the surface. High-resolution spectra of the principle core level of each element present were then acquired for chemical state identification. Both survey and core level XPS spectra were recorded from a surface area of 300 × 700 μm, with such a large area, it is deemed to be representative of the whole sample surface. Data were analysed using the Casa XPS software, using Gaussian–Lorentzian (Voigt) line shapes and Shirley backgrounds.

4.9. Scaffold preparation and equilibration for culture

Scaffolds were prepared for culture by transferring to 70% ethanol and then washed by immersion in phosphate buffered saline (PBS) for 20 min. Scaffolds were centrifuged at 2,000 rpm for 10 min before the removal of PBS and then exposed to ultra violet (UV) radiation for 15 min. The PBS was replaced with 70% ethanol for 2 h at room temperature with rotation. Finally, the scaffolds were washed twice with PBS to remove residual ethanol and stored in StemSpan (Stem Cell Technologies) with 10% foetal calf serum (FCS, Gibco) and penicillin/streptomycin at 100U/0.1 mg per mL of media respectively (Sigma), for at least 2 days to equilibrate at 37 °C with 5% CO_2.

4.10. Three dimensional erythroid cultures

Scaffolds were dried of storage media using sterilised 3 MM Whatman paper and equilibrated to 37 °C until cell seeding. 0.5 × 10^6 CD34$^+$ cells were seeded statically in 20 μl of media, as described below. The scaffolds were then incubated at 37 °C with 5% CO_2 for 2 h; with media added as required to ensure scaffolds did not dry out. 1.5 mL of serum free expansion medium culture media consisting of StemSpan supplemented with; penicillin/streptomycin at 100U/0.1 mg per mL of media respectively (Sigma), cholesterol-rich lipids 40 μg/mL (Sigma), stem cell factor 100 ng/mL (SCF, Miltenyi Biotec), Interleukin-3 1 ng/mL (IL-3, R&D Systems), insulin like growth factor-1 40 ng/mL (IGF-1, R&D Systems), dexamethasone 1 μM/mL (Dex, Sigma) and erythropoietin 2U/mL (Bristol Royal Infirmary) was gently added to each scaffold. Full medium changes were performed every 2 days by lifting the scaffold with tweezers and moving it to a fresh. The cells that are left behind in the well are termed the cell egress, as they have spontaneously exited the scaffold. Scaffold egress was counted using the MACSQuant flow cytometer (Miltenyi Biotec). Cells were auto-labelled

with propidium iodide (Miltenyi Biotec) at a final concentration of 1 μg/mL. Dead cells were excluded, and a live cell count taken as a density per millilitre.

4.11. Three-dimensional neutrophil, macrophage and MSC cultures

For neutrophil cultures, 0.5×10^6 $CD34^+$ cells were isolated and seeded statically in 20 μl of media as described above. Scaffolds were then cultured in IMDM Biochrom (Merck) as a base media supplemented with 10% foetal bovine serum (Gibco), 100 U/mL penicillin (Sigma) and 100 μg/mL streptomycin (Sigma), 50 ng/mL Stem Cell Factor (SCF; Miltenyi Biotec), 10 ng/mL IL-3 (R&D Systems), 50 ng/mL Flt3 ligand (Miltenyi Biotec), 10 ng/mL granulocyte colony stimulating factor (G-CSF, Miltenyi Biotec) and 10 ng/mL granulocyte-macrophage colony stimulating factor (GM-CSF, Miltenyi Biotec). Macrophage cultures were seeded with $CD14^+$ cells isolated from PBMNCs as described above with 0.5×10^6 being seeded onto scaffolds statically. Scaffolds were maintained in media as described above. MSC cultures were initiated with human bone marrow-derived MSCs isolated via adherence selection [38]. Cells were maintained in a DMEM (low glucose, Sigma) base media supplemented with 10% FCS (Gibco), 100 U/mL penicillin (Sigma) and 100 μg/mL streptomycin (Sigma), Glutamax (1/100) and 10 ng/mL fibroblast growth factor (FGF). Scaffolds were cultured with neutrophils for 16 days, MSCs for 21 days, macrophages for 7 days and erythroblasts for 28 days.

4.12. Scale up erythroid culture post 3D culture

Erythroid differentiation post scaffold culture was conducted as previously described [2] and is briefly outlined below. The primary medium was Iscove's Modified Dulbecco's Medium (IMDM; Source BioScience UK Ltd) supplemented with 3U/mL erythropoietin (Epo; Bristol Royal Infirmary), 3 U/mL heparin (Sigma), 0.5 mg/mL holotransferrin (Sigma), 3% (v/v) heat-deactivated Human Male AB Serum (Sigma), 2 mg/mL Human Serum Albumin (HSA; Sigma), 10 μg/mL insulin (Sigma), 100 U/mL penicillin (Sigma) and 100 μg/mL streptomycin (Sigma), with extra supplementation of 100 ng/mL Stem Cell Factor (SCF; Miltenyi Biotec) and 1 ng/mL IL-3 (R&D Systems) to induce cell proliferation. The cells were incubated at 37 °C in 5% CO_2 in this primary medium with daily media addition from Day 3 to Day 7 of culture. From Day 8 to Day 12, secondary medium was added instead, which consisted of the same IMDM base supplemented with only 100 ng/mL SCF. After Day 13, tertiary medium consisting of the IMDM base without growth factor additions was used in order to induce terminal erythroid differentiation. On Day 21, reticulocytes were purified through leukofiltration of the culture to remove nuclei and nucleated cells. For leukofiltration, a leukocyte reduction filter (NHSBT, Filton, Bristol) was pre-soaked and equilibrated with HBSS and the cultured cell suspension was loaded into the filter followed by a large amount of HBSS and allowed to elute by gravity until the flow-through was clear. The resulting flow-through was then centrifuged at 400 g, RT for 20 min and the pelleted cells were resuspended in Phosphate Buffer Saline supplemented with 1 mg/mL Bovine Serum Albumin (BSA; Sigma) and 2 mg/mL glucose (Sigma) (PBSAG).

4.13. Flow cytometry panel

Flow cytometry was performed using 1×10^5 cells labelled with extracellular conjugated antibodies for 30 min at 4 °C. Data were collected using a MacsQuant flow cytometer (Miltenyi Biotec) and processed using FlowJo Version 10.0.7 as previously described [6]. Representative raw flow cytometry data and gating strategies can be found in Supplemental Fig. 4.

4.14. Histology and immunofluorescence

Scaffolds were fixed and prepared for immunofluorescence as previously described [6]. Samples were imaged using a Leica SP5 confocal microscope using a 60× lens (N.A. 1.4) in the Wolfson Bioimaging facility, University of Bristol. Scaffolds were fixed in 4% paraformaldehyde for 15–20 hr and washed four times in PBS for 15 min. Scaffolds were paraffin embedded and sectioned using a Leica RM2125 Microtome into 10 μm sections floated onto polysine slides (VWR). Slides were first baked at 56 °C for approximately 5 hr and then overnight at 37 °C. Slides were de-waxed by immersion into Histo-Clear (National Diagnostics) for 30–45 min before rehydration through a series of graded ethanol. For immunofluorescence, sections were washed once in PBS before blocking with PBS containing 4% BSA (PBSA) for 1 hr. Slides were washed 5 times with PBS before incubating with primary antibody (primary and control antibodies are as stated in figure legends) for 1 hr, again washed 5 times with PBS and incubated with Alexa 647 secondary antibody (Invitrogen) for 1 hr. Slides were washed 5 times in PBS and incubated in DAPI (Thermo Fisher Scientific, formally Molecular Probes) to identify nuclei for 5 min before a further 2 washes. All steps were carried out at room temperature. For coverslips cells were fixed onto slide using 1% paraformaldehyde for 5 min before permeabilisation in 0.05% Triton (in PBS) for 5 min at room temperature. Coverslips were then washed three times and blocked and stained with antibodies as above. Finally, coverslips and slides were washed and mounted using mowiol (Calbiochem). Samples were imaged using a Leica SP5 confocal microscope using a 63× lens (N.A. 1.4) in the Wolfson Bioimaging facility, University of Bristol.

4.15. Scanning electron microscopy

Scaffolds were cut in half and mounted on a chuck with the centre of the scaffold face up. The samples were coated using an Emitech K575X sputter coater with a gold/palladium target and viewed with the Quanta 400FEI Scanning Electron Microscope (SEM) in the Wolfson Bioimaging facility, University of Bristol.

4.16. Cytospin preparation and staining

To analyse cell morphology $5–10 \times 10^4$ cells were resuspended in 100 μL PBS and cytocentrifuged onto slides at 350 g for 5 min (Thermo Scientific, Cytospin 4) before fixation in methanol for 15 min and staining with May-Grünwald's (VWR Chemicals) and Giemsa (Merck Millipore) stains according to manufacturer's instructions.

4.17. ARCA sample preparation and analysis

2×10^6 cells were diluted in 200 μL of a polyvinylpyrrolidone solution (PVP viscosity 28.1 mPa s; Mechatronics Instruments) and samples were assessed in an Automated Rheoscope and Cell Analyser (ARCA) as previously described [46,70]. Deformation index distribution was measured under shear stress and a minimum of 1500 valid cells per sample were acquired.

4.18. Statistical analysis

Where appropriate statistical analysis in the form of a Student's *t*-test, used to determine the level of significance for Fig. 3 and Supplementary Fig. 1b and a one way ANOVA for Fig. 6b. The following indicates, * = $P \leq 0.05$, ** = $P \leq 0.01$, *** = $P \leq 0.001$ in all instances.

4.19. Liquid chromatography mass spectrometry

Scaffolds were prepared and equilibrated as described above and without any cell seeding were taken for mass spectrometry analysis of

proteins deposited during preparation. Scaffolds were then washed 3 times with a boric acid buffer (10 mM boric acid, 154 mM NaCl, 7.2 mM KCl, 1.8 mM $CaCl_2$). Scaffold sections were then cut into 1 mm^2 pieces and resuspended in 50 mM TEAB. The samples were reduced with 20 mM tris(2-carboxyethyl)phosphine (55 °C for 1 hr) and then alkylated using 37.5 mM iodoacetamide (room temperature for 30 min.). The buffer was then removed from the scaffold pieces and any proteins which had been released from the scaffold during these processing steps were precipitated using 6 vol of ice-cold acetone (−20 °C, overnight). Precipitated material was then collected by centrifugation (8000 g for 10 min at 4 °C), resuspended in 100 µl of 50 mM TEAB and transferred back to original scaffold pieces. The samples were then digested using trypsin (2.5 µg, incubated overnight with shaking at 37 °C).

Post digestion, the buffer was removed from each scaffold and desalted using a SepPak cartridge according to the manufacturer's instructions (Waters, Milford, Massachusetts, USA). Eluate from the SepPak cartridge was evaporated to dryness and resuspended in 1% formic acid prior to analysis by nano-LC MSMS using an Orbitrap Fusion Tribrid mass spectrometer (Thermo Scientific). Peptides were fractionated using an Ultimate 3000 nano-LC system in line with an Orbitrap Fusion Tribrid mass spectrometer (Thermo Scientific). In brief, peptides in 1% (vol/vol) formic acid were injected onto an Acclaim PepMap C18 nano-trap column (Thermo Scientific). After washing with 0.5% (vol/vol) acetonitrile 0.1% (vol/vol) formic acid peptides were resolved on a 250 mm × 75 µm Acclaim PepMap C18 reverse phase analytical column (Thermo Scientific) over a 150 min organic gradient, using 7 gradient segments (1–6% solvent B over 1 min., 6–15% B over 58 min., 15–32%B over 58 min., 32–40%B over 5 min., 40–90%B over 1 min., held at 90%B for 6 min and then reduced to 1%B over 1 min.) with a flow rate of 300 nl min^{-1}. Solvent A was 0.1% formic acid and Solvent B was aqueous 80% acetonitrile in 0.1% formic acid. Peptides were ionised by nano-electrospray ionisation at 2.2 kV using a stainless-steel emitter with an internal diameter of 30 µm (Thermo Scientific) and a capillary temperature of 250 °C.

All spectra were acquired using an Orbitrap Fusion Tribrid mass spectrometer controlled by Xcalibur 2.0 software (Thermo Scientific) and operated in data-dependent acquisition mode. FTMS1 spectra were collected at a resolution of 120 000 over a scan range (m/z) of 350–1550, with an automatic gain control (AGC) target of 400 000 and a max injection time of 100 ms. The Data Dependent mode was set to Cycle Time with 3s between master scans. Precursors were filtered according to charge state (to include charge states 2–7), with monoisotopic precursor selection and using an intensity range from 5E3 to 1E20. Previously interrogated precursors were excluded using a dynamic window (40s ± 10 ppm). The MS2 precursors were isolated with a quadrupole mass filter set to a width of 1.6 m/z. ITMS2 spectra were collected with an AGC target of 5000, max injection time of 50 ms and HCD collision energy of 35%.

The raw data files were processed using Proteome Discoverer software v1.4 (Thermo Scientific) and searched against the UniProt Human database (152 927 entries) using the SEQUEST algorithm. Peptide precursor mass tolerance was set at 10 ppm, and MS/MS tolerance was set at 0.6Da. Search criteria included carbamidomethylation of cysteine (+57.0214) as a fixed modification and oxidation of methionine (+15.9949) as a variable modification. Searches were performed with full tryptic digestion and a maximum of 2 missed cleavage events were allowed. The reverse database search option was enabled, and all peptide data was filtered to satisfy false discovery rate (FDR) of 5%.

4.20. Incucyte imaging

Scaffolds were seeded and cultured as described above. The plate was then imaged repeatedly at multiple locations per scaffold culture using the Incucyte Zoom system (Essen BioScience, Welwyn Garden City, UK) every hour at 20× magnification.

Acknowledgements

The authors would like to thank Kate Heesom and Mariangela Wilson at the proteomics facility (University of Bristol) and Rosey Mushens at the International Blood Group Reference Laboratories (IBGRL) for monoclonal antibodies. The authors also thank Pedro Moura for development of the software used to analyse the ARCA data. We also acknowledge the MRC and Wolfson Foundation for establishing the Wolfson Bioimaging Facility (University of Bristol) and for use of confocal microscopes. This work was funded by grants from NIHR Blood and Transfusion Research Unit (NIHR BTRU) in red cell products (NIHR-BTRU-2015-10032) and NHS Blood and Transfusion (NHSBT) R &D (WP15-05).

Appendix A. Supplementary data

Supplementary data to this article can be found online at https://doi.org/10.1016/j.biomaterials.2019.119533.

Author contributions

CES and AMT designed the experiments. CES conducted the majority of the experimental work. AP conducted the scaffold “follow-on” experiments. EAM and CRL provided scaffold materials and EAM functionalised scaffold materials. MW conducted and analysed x-ray photoelectron spectroscopy experiments. DJGG and SGJ provided essential ARCA equipment and software. NRC provided biomaterial expertise. CES and AMT wrote the manuscript and all other authors read and edited the manuscript prior to submission.

Disclaimer

This article presents independent research funded by the National Institute for Health Research (NIHR). The views expressed are those of the authors and not necessarily those of the NHS, the NIHR or the Department of Health and Social Care.

Data availability statement

Data will be made available on request.

References

[1] M.C. Giarratana, H. Rouard, A. Dumont, L. Kiger, I. Safeukui, P.Y. Le Pennec, S. Francois, G. Trugnan, T. Peyrard, T. Marie, S. Jolly, N. Hebert, C. Mazurier, N. Mario, L. Harmand, H. Lapillonne, J.Y. Devaux, L. Douay, Proof of principle for transfusion of in vitro-generated red blood cells, Blood 118 (19) (2011) 5071–5079.
[2] S. Kupzig, S.F. Parsons, E. Curnow, D.J. Anstee, A. Blair, Superior survival of ex vivo cultured human reticulocytes following transfusion into mice, Haematologica 102 (3) (2017) 476–483.
[3] T. Jozaki, K. Aoki, H. Mizumoto, T. Kajiwara, In vitro reconstruction of a three-dimensional mouse hematopoietic microenvironment in the pore of polyurethane foam, Cytotechnology 62 (6) (2010) 531–537.
[4] T.M. Blanco, A. Mantalaris, A. Bismarck, N. Panoskaltsis, The development of a three-dimensional scaffold for ex vivo biomimicry of human acute myeloid leukaemia, Biomaterials 31 (8) (2010) 2243–2251.
[5] T. Mortera-Blanco, A. Mantalaris, A. Bismarck, N. Aqel, N. Panoskaltsis, Long-term cytokine-free expansion of cord blood mononuclear cells in three-dimensional scaffolds, Biomaterials 32 (35) (2011) 9263–9270.
[6] C.E. Severn, H. Macedo, M.J. Eagle, P. Rooney, A. Mantalaris, A.M. Toye, Polyurethane scaffolds seeded with CD34(+) cells maintain early stem cells whilst also facilitating prolonged egress of haematopoietic progenitors, Sci. Rep. 6 (2016) 32149.
[7] M.S. Ferreira, W. Jahnen-Dechent, N. Labude, M. Bovi, T. Hieronymus, M. Zenke, R.K. Schneider, S. Neuss, Cord blood-hematopoietic stem cell expansion in 3D fibrin scaffolds with stromal support, Biomaterials 33 (29) (2012) 6987–6997.
[8] J. Tan, T. Liu, L. Hou, W. Meng, Y. Wang, W. Zhi, L. Deng, Maintenance and expansion of hematopoietic stem/progenitor cells in biomimetic osteoblast niche, Cytotechnology 62 (5) (2010) 439–448.
[9] Y. Li, T. Ma, D.A. Kniss, S.T. Yang, L.C. Lasky, Human cord cell hematopoiesis in three-dimensional nonwoven fibrous matrices: in vitro simulation of the marrow microenvironment, J. Hematother. Stem Cell Res. 10 (3) (2001) 355–368.

[10] Y. Tomimori, M. Takagi, T. Yoshida, The construction of an in vitro three-dimensional hematopoietic microenvironment for mouse bone marrow cells employing porous carriers, Cytotechnology 34 (1–2) (2000) 121–130.
[11] M.C. Allenby, N. Panoskaltsis, A. Tahlawi, S.B. Dos Santos, A. Mantalaris, Dynamic human erythropoiesis in a three-dimensional perfusion bone marrow biomimicry, Biomaterials 188 (2019) 24–37.
[12] A. Raic, L. Rodling, H. Kalbacher, C. Lee-Thedieck, Biomimetic macroporous PEG hydrogels as 3D scaffolds for the multiplication of human hematopoietic stem and progenitor cells, Biomaterials 35 (3) (2014) 929–940.
[13] M.P. Lutolf, J.L. Lauer-Fields, H.G. Schmoekel, A.T. Metters, F.E. Weber, G.B. Fields, J.A. Hubbell, Synthetic matrix metalloproteinase-sensitive hydrogels for the conduction of tissue regeneration: engineering cell-invasion characteristics, Proc. Natl. Acad. Sci. U.S.A 100 (9) (2003) 5413–5418.
[14] M.L. Cuchiara, S. Coskun, O.A. Banda, K.L. Horter, K.K. Hirschi, J.L. West, Bioactive poly(ethylene glycol) hydrogels to recapitulate the HSC niche and facilitate HSC expansion in culture, Biotechnol. Bioeng. 113 (4) (2016) 870–881.
[15] L. Rodling, A. Raic, C. Lee-Thedieck, Fabrication of biofunctionalized, cell-laden macroporous 3D PEG hydrogels as bone marrow analogs for the cultivation of human hematopoietic stem and progenitor cells, Methods Mol. Biol. 1202 (2014) 121–130.
[16] L. Rodling, E.M. Volz, A. Raic, K. Brandle, M. Franzreb, C. Lee-Thedieck, Magnetic macroporous hydrogels as a novel approach for perfused stem cell culture in 3D scaffolds via contactless motion control, Adv. Healthc. Mater. 7 (9) (2018) e1701403.
[17] D.J. Anstee, A. Gampel, A.M. Toye, Ex-vivo generation of human red cells for transfusion, Curr. Opin. Hematol. 19 (3) (2012) 163–169.
[18] N.R. Cameron, High internal phase emulsion templating as a route to well-defined porous polymers, Polymer 46 (5) (2005) 1439–1449.
[19] M.S. Silverstein, Emulsion-templated porous polymers: a retrospective perspective, Polymer 55 (1) (2014) 304–320.
[20] M.S. Silverstein, PolyHIPEs: recent advances in emulsion-templated porous polymers, Prog. Polym. Sci. 39 (1) (2014) 199–234.
[21] I. Pulko, P. Krajnc, High internal phase emulsion templating–a path to hierarchically porous functional polymers, Macromol. Rapid Commun. 33 (20) (2012) 1731–1746.
[22] S.D. Kimmins, N.R. Cameron, Functional porous polymers by emulsion templating: recent advances, Adv. Funct. Mater. 21 (2) (2011) 211–225.
[23] M.S. Silverstein, N.R. Cameron, M.A. Hillmyer, Porous Polymers, Wiley-Blackwell, Oxford, 2011.
[24] G. Akay, M.A. Birch, M.A. Bokhari, Microcellular polyHIPE polymer supports osteoblast growth and bone formation in vitro, Biomaterials 25 (18) (2004) 3991–4000.
[25] M.A. Bokhari, G. Akay, S. Zhang, M.A. Birch, The enhancement of osteoblast growth and differentiation in vitro on a peptide hydrogel-polyHIPE polymer hybrid material, Biomaterials 26 (25) (2005) 5198–5208.
[26] M. Bokhari, R.J. Carnachan, N.R. Cameron, S.A. Przyborski, Culture of HepG2 liver cells on three dimensional polystyrene scaffolds enhances cell structure and function during toxicological challenge, J. Anat. 211 (4) (2007) 567–576.
[27] M.W. Hayman, K.H. Smith, N.R. Cameron, S.A. Przyborski, Enhanced neurite outgrowth by human neurons grown on solid three-dimensional scaffolds, Biochem. Biophys. Res. Commun. 314 (2) (2004) 483–488.
[28] M.W. Hayman, K.H. Smith, N.R. Cameron, S.A. Przyborski, Growth of human stem cell-derived neurons on solid three-dimensional polymers, J. Biochem. Biophys. Methods 62 (3) (2005) 231–240.
[29] E.A. Neofytou, E. Chang, B. Patloia, L.M. Joubert, J. Rajadas, S.S. Gambhir, Z. Cheng, R.C. Robbins, R.E. Beygui, Adipose tissue-derived stem cells display a proangiogenic phenotype on 3D scaffolds, J. Biomed. Mater. Res. A 98a (3) (2011) 383–393.
[30] A.R. Murphy, I. Ghobrial, P. Jamshidi, A. Laslett, C.M. O'Brien, N.R. Cameron, Tailored emulsion-templated porous polymer scaffolds for iPSC-derived human neural precursor cell culture, Polym. Chem.-Uk 8 (43) (2017) 6617–6627.
[31] A.M. Eissa, F.S.V. Barros, P. Vrljicak, J.J. Brosens, N.R. Cameron, Enhanced differentiation potential of primary human endometrial cells cultured on 3D scaffolds, Biomacromolecules 19 (8) (2018) 3343–3350.
[32] A.S. Hayward, A.M. Eissa, D.J. Maltman, N. Sano, S.A. Przyborski, N.R. Cameron, Galactose-functionalized polyHIPE scaffolds for use in routine three dimensional culture of mammalian hepatocytes, Biomacromolecules 14 (12) (2013) 4271–4277.
[33] A.S. Hayward, N. Sano, S.A. Przyborski, N.R. Cameron, Acrylic-acid-functionalized PolyHIPE scaffolds for use in 3D cell culture, Macromol. Rapid Commun. 34 (23–24) (2013) 1844–1849.
[34] S.A. Richardson, T.M. Rawlings, J. Muter, M. Walker, J.J. Brosens, N.R. Cameron, A.M. Eissa, Covalent attachment of fibronectin onto emulsion-templated porous polymer scaffolds enhances human endometrial stromal cell adhesion, infiltration, and function, Macromol. Biosci. 19 (2) (2019) e1800351.
[35] S. Caldwell, D.W. Johnson, M.P. Didsbury, B.A. Murray, J.J. Wu, S.A. Przyborski, N.R. Cameron, Degradable emulsion-templated scaffolds for tissue engineering from thiol-ene photopolymerisation, Soft Matter 8 (40) (2012) 10344–10351.
[36] C.Y. Chen, A.M. Eissa, T.L. Schiller, N.R. Cameron, Emulsion-templated porous polymers prepared by thiol-ene and thiol-yne photopolymerisation using multifunctional acrylate and non-acrylate monomers, Polymer 126 (2017) 395–401.
[37] A.M. Eissa, P. Wilson, C. Chen, J. Collins, M. Walker, D.M. Haddleton, N.R. Cameron, Reversible surface functionalisation of emulsion-templated porous polymers using dithiophenol maleimide functional macromolecules, Chem. Commun. 53 (70) (2017) 9789–9792.
[38] R.C. Deller, T. Richardson, R. Richardson, L. Bevan, I. Zampetakis, F. Scarpa, A.W. Perriman, Artificial cell membrane binding thrombin constructs drive in situ fibrin hydrogel formation, Nat. Commun. 10 (1) (2019) 1887.
[39] V. Tirelli, B. Ghinassi, A.R. Migliaccio, C. Whitsett, F. Masiello, M. Sanchez, G. Migliaccio, Phenotypic definition of the progenitor cells with erythroid differentiation potential present in human adult blood, Stem Cell. Int. 2011 (2011) 602483.
[40] D. Ward, D. Carter, M. Homer, L. Marucci, A. Gampel, Mathematical Modelling Reveals Differential Effects of Erythropoietin on Proliferation and Lineage Commitment of Human Hematopoietic Progenitors in Early Erythroid Culture, Haematologica, (2015).
[41] E. Heideveld, F. Masiello, M. Marra, F. Esteghamat, N. Yagci, M. von Lindern, A.R. Migliaccio, E. van den Akker, CD14+ Cells from Peripheral Blood Positively Regulate Hematopoietic Stem and Progenitor Cell Survival Resulting in Increased Erythroid Yield, Haematologica, (2015).
[42] O. Klimchenko, M. Mori, A. Distefano, T. Langlois, F. Larbret, Y. Lecluse, O. Feraud, W. Vainchenker, F. Norol, N. Debili, A common bipotent progenitor generates the erythroid and megakaryocyte lineages in embryonic stem cell-derived primitive hematopoiesis, Blood 114 (8) (2009) 1506–1517.
[43] J.E. Rasko, E. O'Flaherty, C.G. Begley, Mpl ligand (MGDF) alone and in combination with stem cell factor (SCF) promotes proliferation and survival of human megakaryocyte, erythroid and granulocyte/macrophage progenitors, Stem cells 15 (1) (1997) 33–42.
[44] P. Halle, C. Rouzier, J. Kanold, N. Boiret, C. Rapatel, G. Mareynat, A. Tchirkov, M. Berger, P. Travade, J. Bonhomme, F. Demeocq, Ex vivo expansion of CD34+/CD41+ late progenitors from enriched peripheral blood CD34+ cells, Ann. Hematol. 79 (1) (2000) 13–19.
[45] E. Belay, C.P. Miller, A.N. Kortum, B. Torok-Storb, C.A. Blau, D.W. Emery, A hyperactive Mpl-based cell growth switch drives macrophage-associated erythropoiesis through an erythroid-megakaryocytic precursor, Blood 125 (6) (2015) 1025–1033.
[46] J.G. Dobbe, G.J. Streekstra, M.R. Hardeman, C. Ince, C.A. Grimbergen, Measurement of the distribution of red blood cell deformability using an automated rheoscope, Cytometry 50 (6) (2002) 313–325.
[47] C.R. Langford, D.W. Johnson, N.R. Cameron, Chemical functionalization of emulsion-templated porous polymers by thiol-ene "click" chemistry, Polym Chem-Uk 5 (21) (2014) 6200–6206.
[48] R.C. Sainson, J. Aoto, M.N. Nakatsu, M. Holderfield, E. Conn, E. Koller, C.C. Hughes, Cell-autonomous notch signaling regulates endothelial cell branching and proliferation during vascular tubulogenesis, FASEB J. 19 (8) (2005) 1027–1029.
[49] J. Lee, N.A. Kotov, Notch ligand presenting acellular 3D microenvironments for ex vivo human hematopoietic stem-cell culture made by layer-by-layer assembly, Small 5 (9) (2009) 1008–1013.
[50] P. Benveniste, P. Serra, D. Dervovic, E. Herer, G. Knowles, M. Mohtashami, J.C. Zuniga-Pflucker, Notch signals are required for in vitro but not in vivo maintenance of human hematopoietic stem cells and delay the appearance of multipotent progenitors, Blood 123 (8) (2014) 1167–1177.
[51] R.L.L. Moore, M.J. Worrallo, P.D. Mitchell, J. Harriman, K.E. Glen, R.J. Thomas, Immobilisation of Delta-like 1 ligand for the scalable and controlled manufacture of hematopoietic progenitor cells in a stirred bioreactor, BMC Biotechnol. 17 (1) (2017) 65.
[52] D. Kratzer, A. Ludwig-Husemann, K. Junges, U. Geckle, C. Lee-Thedieck, Nanostructured bifunctional hydrogels as potential instructing platform for hematopoietic stem cell differentiation, Front. Mater. 5 (2019).
[53] C. Lee-Thedieck, N. Rauch, R. Fiammengo, G. Klein, J.P. Spatz, Impact of substrate elasticity on human hematopoietic stem and progenitor cell adhesion and motility, J. Cell Sci. 125 (Pt 16) (2012) 3765–3775.
[54] A. Raic, T. Naolou, A. Mohra, C. Chatterjee, C. Lee-Thedieck, 3D models of the bone marrow in health and disease: yesterday, today and tomorrow, MRS Commun. 9 (1) (2019) 37–52.
[55] A. Buxboim, K. Rajagopal, A.E. Brown, D.E. Discher, How deeply cells feel: methods for thin gels, J. Phys. Condens. Matter 22 (19) (2010) 194116.
[56] J. Holst, S. Watson, M.S. Lord, S.S. Eamegdool, D.V. Bax, L.B. Nivison-Smith, A. Kondyurin, L. Ma, A.F. Oberhauser, A.S. Weiss, J.E. Rasko, Substrate elasticity provides mechanical signals for the expansion of hemopoietic stem and progenitor cells, Nat. Biotechnol. 28 (10) (2010) 1123–1128.
[57] A. Subramanian, H.Y. Lin, Crosslinked chitosan: its physical properties and the effects of matrix stiffness on chondrocyte cell morphology and proliferation, J. Biomed. Mater. Res. A 75 (3) (2005) 742–753.
[58] W. Xu, B.Z. Molino, F. Cheng, P.J. Molino, Z. Yue, D. Su, X. Wang, S. Willfor, C. Xu, G.G. Wallace, On low-concentration inks formulated by nanocellulose assisted with gelatin methacrylate (GelMA) for 3D printing toward wound healing application, ACS Appl. Mater. Interfaces 11 (9) (2019) 8838–8848.
[59] L.E. McNamara, R. Burchmore, M.O. Riehle, P. Herzyk, M.J. Biggs, C.D. Wilkinson, A.S. Curtis, M.J. Dalby, The role of microtopography in cellular mechanotransduction, Biomaterials 33 (10) (2012) 2835–2847.
[60] A.B. Bello, H. Park, S.H. Lee, Current approaches in biomaterial-based hematopoietic stem cell niches, Acta Biomater. 72 (2018) 1–15.
[61] H. Donnelly, M. Salmeron-Sanchez, M.J. Dalby, Designing stem cell niches for differentiation and self-renewal, J. R. Soc. Interface 15 (145) (2018).
[62] M. Salwiczek, Y. Qu, J. Gardiner, R.A. Strugnell, T. Lithgow, K.M. McLean, H. Thissen, Emerging rules for effective antimicrobial coatings, Trends Biotechnol. 32 (2) (2014) 82–90.
[63] P. Caliceti, F.M. Veronese, Pharmacokinetic and biodistribution properties of poly(ethylene glycol)-protein conjugates, Adv. Drug Deliv. Rev. 55 (10) (2003) 1261–1277.
[64] A.J. Bell, T.J. Satchwell, K.J. Heesom, B.R. Hawley, S. Kupzig, M. Hazell,

R. Mushens, A. Herman, A.M. Toye, Protein distribution during human erythroblast enucleation in vitro, PLoS One 8 (4) (2013) e60300.
[65] E. van den Akker, T.J. Satchwell, S. Pellegrin, G. Daniels, A.M. Toye, The majority of the in vitro erythroid expansion potential resides in CD34(-) cells, outweighing the contribution of CD34(+) cells and significantly increasing the erythroblast yield from peripheral blood samples, Haematologica 95 (9) (2010) 1594–1598.
[66] R.E. Griffiths, S. Kupzig, N. Cogan, T.J. Mankelow, V.M. Betin, K. Trakarnsanga, E.J. Massey, S.F. Parsons, D.J. Anstee, J.D. Lane, The ins and outs of human reticulocyte maturation: autophagy and the endosome/exosome pathway, Autophagy 8 (7) (2012) 1150–1151.
[67] E. van den Akker, T.J. Satchwell, S. Pellegrin, J.F. Flatt, M. Maigre, G. Daniels, J. Delaunay, L.J. Bruce, A.M. Toye, Investigating the key membrane protein changes during in vitro erythropoiesis of protein 4.2 (-) cells (mutations Chartres 1 and 2), Haematologica 95 (8) (2010) 1278–1286.
[68] J.L. Ratcliffe, M. Walker, A.M. Eissa, S. Du, S.A. Przyborski, A.L. Laslett, N.R. Cameron, Optimized peptide functionalization of thiol-acrylate emulsion--templated porous polymers leads to expansion of human pluripotent stem cells in 3D culture, J. Polym. Sci. A Polym. Chem. 57 (2019) 1974–1981.
[69] A. Barbetta, N.R. Cameron, Morphology and surface area of emulsion-derived (PolyHIPE) solid foams prepared with oil-phase soluble porogenic solvents: three-component surfactant system, Macromolecules 37 (9) (2004) 3202–3213.
[70] P.L. Moura, B.R. Hawley, T.J. Mankelow, R.E. Griffiths, J.G.G. Dobbe, G.J. Streekstra, D.J. Anstee, T.J. Satchwell, A.M. Toye, Non-muscle Myosin II Drives Vesicle Loss during Human Reticulocyte Maturation, Haematologica, (2018).